Theoretical study of the interstice statistics of the oxygen sublattice in vitreous SiO_2

S. L. Chan and S. R. Elliott
Department of Physical Chemistry, University of Cambridge, Lensfield Road, Cambridge CB2 1EP, England
(Received 6 July 1990)

The interstice statistics of the oxygen sublattice of the canonical inorganic glass-former silica have been investigated theoretically for a number of structural models of v-SiO_2. It is found that spheres with radii smaller than 2.41 Å minus the oxygen radius can travel freely through a model of v-SiO_2 made by Feuston and Garofalini. The nonoverlapping interstice size distribution can be described by a log-normal function. The concentrations of interstitial sites in these models with radii greater than the size of rare-gas atoms agree with the experimental values from gas-solubility studies.

I. INTRODUCTION

Models for the structure of amorphous materials are usually characterized in terms of atom-atom pair-correlation functions since these quantities can be obtained directly from diffraction experiments. However, instead of concentrating on the atomic network, an alternative approach is to analyze such structural models in terms of the network of voids or interstices between the atoms. Such an approach is particularly appropriate for the case of those structures which can be regarded as being comprised of a densely packed arrangement of spheres, as in the dense-random-packed (DRP) models constructed to simulate the structures of simple liquids and amorphous metals.[1-3] Indeed, a considerable effort has been made[4-8] to analyze DRP structures in terms of their interstice statistics. Furthermore, the interconnection of interstices via "saddle-point doorways"[9,10] and their percolation behavior[8,10] have also been investigated with mass-transport (interstitial diffusion) processes in mind.

However, models of structures with directional (i.e., covalent) bonding have very rarely been investigated in terms of the interstice network. Popescu[11] has investigated the size distribution of interstices in nonperiodic (and hence small effective volume) continuous-random-network (CRN) models of amorphous Ge, As, $CdGeAs_2$, As_2Se_3, $GdFe_3$, $GdCo_3Mo_{0.5}$, and $GeAs_2Te_7$, and Mitra and Hockney[12] have also obtained the interstice size distribution for a model of v-SiO_2 produced by molecular-dynamics simulation.

The aim of this paper is to discuss the interstice statistics of models for the structure of the archetypal covalent glass-forming system, namely SiO_2, using the theoretical approach which we have developed recently for the case of DRP structures.

II. SILICA AS A QUASI-DENSE-PACKED STRUCTURE

The structures of crystalline and vitreous forms of silica are usually considered in covalent bonding terms, i.e., as a network of Si—O bonds in which Si is tetrahedrally coordinated by O atoms and O atoms are bonded to two Si atoms. They are usually regarded as comprising a network of interconnected $SiO_{4/2}$ coordination polyhedra which are joined through their apices. Such a picture is the basis for the Zachariasen[13] philosophy for the structure of covalent network glasses (see Galeener[14] for a review), and a number of CRN models for the structure of v-SiO_2 have been constructed on this basis (e.g., see Refs. 15 and 16).

Nevertheless, under certain circumstances it is also profitable to consider the structure of silica and silicates in terms of a quasi-dense-packed arrangement (of the oxygen sublattice). Gaskell[17] and Eckersley and Gaskell[18] have emphasized the usefulness of this picture for the case of alkali silicates, where considerations of the density indicate the existence of a close-packed arrangement of oxygen atoms around the network-modifying cations. However, a number of features indicate that the structure of vitreous silica itself can also be regarded in terms of a quasi-dense-packed arrangement of oxygen atoms.

Both Thathachari and Tiller[19,20] and Galeener[21] have demonstrated that the skewed Si—O—Si bond-angle distribution, $P(\theta_O)$, in v-SiO_2, centered on the most probable angle $\theta_O^M \simeq 145°$, as obtained from x-ray-diffraction data[22] and magic-angle spinning nuclear-magnetic-resonance spectra,[23] appears to arise principally from *steric* constraints, in particular from the existence of a minimum oxygen-oxygen separation $D_{O\text{-}O}^{\min}$ between oxygen atoms in different $SiO_{4/2}$ tetrahedra. Using an analytic treatment, Galeener[21] found that the best fit to the experimental distribution $P(\theta_O)$ was achieved for a ratio $D_{O\text{-}O}^{\min}/r_{Si\text{-}O} = 1.95$ or, taking the nearest-neighbor Si—O bond length to be $r_{Si\text{-}O} = 1.60$ Å, for $D_{O\text{-}O}^{\min} = 3.12$ Å. This might be taken to imply that the oxygen radius is about 1.56 Å.

It is interesting to evaluate the packing density η_O of the oxygen sublattice, defined as

$$\eta_O = \frac{4\pi R_O^3}{3V_O} , \tag{1}$$

TABLE I. Oxygen sublattice packing density η_O as a function of oxygen radius R_O in Feuston and Garofalini's model of vitreous SiO_2. In order to make comparisons with previous results on a DRP (Ref. 10), a value of 1.51 Å, within Bondi's limits of van der Waals radius, is chosen for R_O for most results reported here. The packing density of our DRP is 0.634.

η_O	R_O (Å)	Structural origin
0.424	1.32	Half intratetrahedral O-O separation[a]
0.574	1.46	Lower limit of the van der Waals radius obtained by Bondi[b]
0.635	1.51	Value chosen in this study
0.648	1.52	Upper limit of the van der Waals radius obtained by Bondi[b]
0.701	1.56	Half minimum nonbonded O-O separation[c]

[a]Reference 17.
[b]Reference 24.
[c]Reference 21.

where R_O is the effective radius of the oxygen atom and V_O is the average volume per oxygen atom in the structure. Table I gives the packing density η_O as a function of various chosen values of R_O. Note that a choice of 1.51 Å for R_O leads to a packing density very near to that of a DRP structure.[10] Since comparisons will frequently be made with the results of a DRP structure,[10] and because the value of 1.51 Å lies within the limits of the van der Waals radius obtained by Bondi,[24] and not far (only 3% difference) from the oxygen radius deduced by Galeener,[21] it is convenient to pick 1.51 Å as the oxygen radius. Note that the O-O distance within a $SiO_{4/2}$ tetrahedron is only about 2.64 Å. With an oxygen radius of 1.51 Å (or in fact any value above 1.32 Å), the oxygen atoms within a $SiO_{4/2}$ tetrahedron will overlap. Thus the oxygen sublattice should be considered as a soft-sphere rather than a hard-sphere packing.

In conclusion, it is reasonable to regard the oxygen sublattice of v-SiO_2 as being represented by a soft-sphere packing. However, it should be recognized that this picture is only approximate, since it is clear that in fact there are *two* types of nearest-neighbor oxygen atoms (those bridged by Si atoms and those which are not), and this would mean that two different force laws should determine their separations. Nevertheless, there is much compelling evidence (see above) that in fact purely geometric packing considerations control for the most part the topology of the oxygen sublattice.

III. EXPERIMENTAL EVIDENCE FOR INTERSTICES IN v-SiO_2

By definition, interstices are those voids in a structure which are comparable in size to, or smaller than, the largest atoms present. In concentrating entirely on the interstice statistics, therefore, it is assumed that the structure of the material is sufficiently nondefective that larger voids (of the size of several atoms) are not present. Small-angle (neutron or x-ray) scattering is sensitive to larger-sized voids (say greater than 10 Å) because then the scattering intensity is confined to values of scattering vector $\mathbf{Q}$ considerably *smaller* than that of the first peak in the atomic interference function [structure factor, $S(\mathbf{Q})$], typically lying at $Q \simeq 1$–2 Å^{-1}. However, small-angle scattering from the atomic-sized or smaller voids (interstices) of interest here would extend to much larger values of $\mathbf{Q}$ and hence such scattering intensity would lie beneath that of $S(\mathbf{Q})$ and correspondingly be unobservable.

Although diffraction cannot be used as a probe for the structure of interstices, the diffusion and solubility of gases in the material can be used as a probe for (a subset of) the interstitial volume. A number of such studies have been performed for v-SiO_2 using the rare-gas atoms He and Ne (Refs. 25–33) as well as using H_2 and D_2.[34] Some crystalline polymorphs of silica (tridymite and cristobalite) have also been studied in this way.[35] The permeability K of a gas can be obtained from a measurement of the steady-state flow rate through a membrane of the material under a pressure gradient, and the diffusivity D is obtained either by monitoring the approach to steady state at the beginning of a permeation experiment or by monitoring gas evolution from the membrane at the end of such an experiment. These quantities can be combined to give an estimate for the solubility S of the gas in question via the relation

$$K = DS \ . \tag{2}$$

The concentration of solubility sites in the material occupied by the probe gas atoms can only be obtained from the experimentally obtained values of S by using a model for the gas solubility. Both the Langmuir adsorption isotherm model[27,35] and a statistical-mechanical model treating the dissolved gas atoms or molecules as three-dimensional isotropic harmonic oscillators[25,36] have been used, and they give similar results.[30] Estimates for the concentrations of solubility sites N_S for the gases He, Ne, and D_2 in v-SiO_2 are given in Table II (after Shelby[30]).

There is a distinct trend for N_S to decrease as the size of the probe atom increases (e.g., from He to Ne), which is evidence for a rather wide distribution of interstice sizes; the number of sites accessible to the larger gas atoms is obviously smaller than that accessible to smaller-sized probe atoms. The spread in results for a particular probe gas (and a given method of analysis) probably arises from subtle differences in the interstice distribution of the glasses resulting from differing thermal treatments; it appears that a systematic study of gas solubility in variously heat-treated glasses has not yet been carried out to investigate the correlation between interstice statistics and annealing-induced structural relaxa-

TABLE II. Solubility site concentrations N_S for various gases in v-SiO_2 [after Shelby (Ref. 30)]. The dagger denotes values obtained assuming a vibrational statistical-mechanical model and the asterisk the Langmuir adsorption isotherm model.

	He	Ne	D_2
N_S (10^{21} cm^{-3})	1.8–3.3†	1.06†	1.27†
	1.9*	1.3*	1.07*

tion. In an extended analysis of these data, Shackelford[31–33] has taken representative values to be $N_S = 2.3 \times 10^{21}$ cm^{-3} (He) and 1.3×10^{21} cm^{-3} (Ne).

In addition to being another method of characterizing noncrystalline structures, a knowledge of the interstice statistics of (silica) glass is important for certain technological reasons. The relatively high permeability of these materials to gases such as He, Ne, and H_2, etc., intimately connected with the size distribution and connectivity of interstices in the structure, places certain restrictions on the use of such materials in high-vacuum applications.[30] In addition, the technologically very important process of the thermal oxidation of crystalline Si to form an insulating oxide layer is believed to be controlled, for the most part, by the diffusion of oxygen molecules (or perhaps atoms, depending on the conditions) through the growing amorphous silica film.[37,38] Finally, the diffusion behavior of inert gases in glasses may shed light on the transport properties of ions in the same materials.[39]

IV. METHOD OF ANALYSIS OF INTERSTICE STATISTICS

The methods used to investigate the interstice statistics, connectivity, and percolation behavior of structural models of v-SiO_2 reported in this paper were essentially the same as those developed previously to study these quantities in DRP models. In brief, this approach links interstices, diffusion saddle-point doorways, and free volume. The analysis method was applied only to the oxygen sublattice, the Si atoms being regarded as occupying regular tetrahedral interstices in this quasi-dense-packed arrangement (and this has been checked to be the case). In this sense, the analysis is very similar to that of the single-component DRP model reported previously.[10]

Interstices were identified by finding the equidistance point Q for all sets of four nearby atoms A, B, C, and D subject to the condition that no atoms closer to Q than A, B, C, or D exist and the α's in the equation

$$\alpha_1 \mathbf{QA} + \alpha_2 \mathbf{QB} + \alpha_3 \mathbf{QC} + \alpha_4 \mathbf{QD} = \mathbf{0} \tag{3}$$

all have the same sign.

Doorways between interstices were identified with those triangular arrangements of atoms ABC for which the circumcenter P (on the plane ABC) has no atoms nearer to it than A, B, or C. (Doorways that do not satisfy this simple criterion are discussed in Ref. 10.) Then, all compartments enclosed by these doorways are found and, ideally, each compartment should correspond to an interstice. In practice, because of ambiguities connected with the identification of whether or not particular triangular arrangements behave as doorways, not every compartment was found to contain an interstice, although none contained more than one interstice. Since these compartments correspond to the coordination polyhedra of the interstices, the atomic coordination number of an interstice is simply the number of vertices of its corresponding compartment, and hence no arbitrary cutoff distance criterion for neighboring atoms need be invoked as in most previous studies on interstices.[4,6,7]

The analysis outlined above finds *all* interstices, including those which overlap each other. The subset of *nonoverlapping* interstices was identified in the following way. All interstices were sorted according to their sizes, and interstitial spheres were inserted sequentially, starting from the largest interstice. If a sphere of the size of the interstice could not be inserted (because it would otherwise overlap with a previously inserted sphere in a neighboring interstice), the interstices were deemed to overlap and the smaller interstice of the two was discarded.

The free volume and percolation behavior of the interstice network can then be readily obtained using these definitions of interstices and doorways. For a given probe-atom radius, all compartments containing interstices whose radii are larger than that of the probe are connected to other such compartments via those doorways whose sizes are also larger than that of the probe. Each cluster of such connected compartments then corresponds to a patch of free volume. Percolation behavior through the interstice network of a model can be investigated *approximately* by evaluating the compartment cluster size as a function of the size of the probe atom. Alternatively, for models with periodic boundary conditions, the percolation condition (infinite cluster) can be evaluated *exactly* by finding the probe size for which at least one of the interstice sites is linked to its image outside the box.

It should be noted that, using this method of interstice analysis, some quantities (e.g., total number of interstitial sites and doorways, and interstice coordination) are *independent* of the choice of the radius R_O of the oxygen atoms, whereas other quantities (notably the number of nonoverlapping interstices and the critical probe radius for percolation) are dependent on R_O.

V. MODELS INVESTIGATED

The model for v-SiO_2 that has been investigated in detail in this study was built by Feuston and Garofalini[40] using molecular dynamics (MD) and employing an interatomic potential containing both two-body (Coulombic) terms and a three-body (bond-bending) term to simulate covalent effects. The model consists of 216 Si and 432 O atoms in a cubic box of side 21.40 Å with periodic boundary conditions. The mean Si—O bond length is 1.62 Å and the average Si—O—Si bond angle is $\theta_O^m = 154.2°$. *Unless stated otherwise, results in Sec. VI are obtained from this model, which will be denoted as the FG model.*

The other v-SiO_2 models investigated include a computer-generated CRN cluster built by serial addition of atoms by Gladden,[16] a periodic boundary model constructed by decorating an a-Si model by Ching,[41] a model built by a Monte Carlo method by Guttman and Rahman,[42] and a molecular-dynamics model built by Alvarez *et al.*[43]

Whenever comparisons are made with a DRP model, the DRP model used is the one we built by a condensed-gas method[10] *unless stated otherwise.* In order to make comparisons between the oxygen sublattice and the DRP model, the oxygen atom radius R_O was chosen to be 1.51 Å (see Sec. II) so that the two packings will have similar densities.

VI. RESULTS

In the FG model, we have identified a total of 1157 interstitial sites in the oxygen sublattice. This is equivalent to 2.68 sites per O atom, which is considerably lower than the value of 5.13 sites per atom found previously for a DRP structure. Included in these 1157 sites are 216 tetrahedral sites otherwise occupied by the Si atoms; removal of these leaves 941 true interstitial sites (including overlapping sites—see later), or equivalently 2.18 true interstices per O atom or 4.36 sites per SiO_2 unit. The total number of true interstices per oxygen atom is surprisingly similar for all the models which we have examined (see Table III).

The set of nonoverlapping interstices in the oxygen sublattice was identified using the procedure outlined in Sec. IV. Figure 1(a) shows the size distributions for all interstices and the nonoverlapping subset (excluding in both cases the Si-containing sites). As mentioned previously, nonoverlapping interstices can only be identified following the choice of a particular value for the oxygen atom radius R_O. A value of $R_O = 1.51$ Å (see Sec. II) has been taken, leading to a nonoverlapping subset of 447 interstices (1.03 per O atom, or 2.06 per unit of SiO_2). In fact, the *shape* of the size distribution of nonoverlapping interstices is not particularly sensitive to small variations in R_O, although obviously the origin of the length scale of the distribution does depend on the value of R_O taken. A discussion of how the choice of R_O affects the number of nonoverlapping interstices will be continued in Sec. VII. From Fig. 1(a), it can be seen that, as expected, the size distribution of nonoverlapping interstices is appreciably smaller than that for all interstices, since many of the interstices in the latter case are comprised, in fact, of overlapping sites.

The value of 2.06 nonoverlapping interstices per SiO_2 unit in the FG model is considerably higher than the corresponding value of 1.00 in high cristobalite.[12] However, the cristobalite interstices are quite large—half of them can accommodate atoms of radii up to 1.21 Å while the other half can accommodate atoms of radii up to 1.15 Å (taking $R_O = 1.51$ Å). This is not difficult to understand. High cristobalite is crystalline: its atoms are arranged in an orderly way, and so must the free volume. The free-volume regions combine to form larger but fewer interstices.

Shown in Fig. 1(b) is a comparison of the nonoverlapping interstice size distribution for the oxygen sublattice of v-SiO_2 and for the DRP model. For a fair comparison of the packings, Si-containing sites are also included for

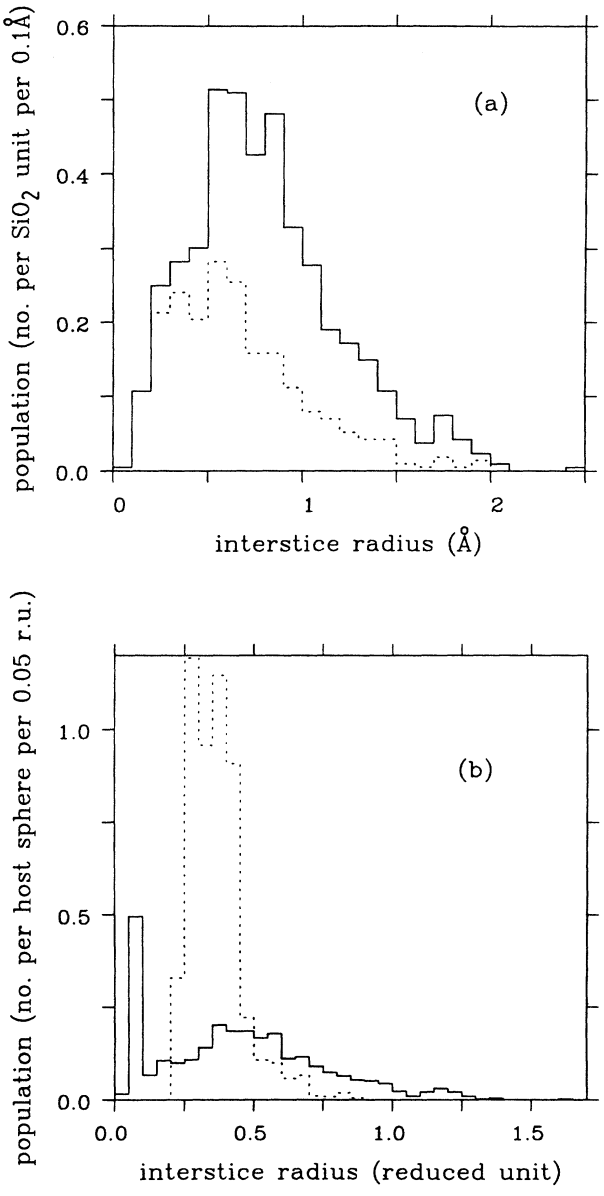

FIG. 1. Interstice size distributions. (a) Interstice size distribution of the oxygen sublattice of the FG model (Feuston and Garofalini, Ref. 40) is plotted, excluding the Si-containing sites. The solid line represents all interstices while the dashed line represents nonoverlapping sites only. The oxygen radius is taken to be 1.51 Å. (b) Comparison with the results for a DRP. The solid line represents the distribution of all interstices, including those containing Si atoms and also overlapping ones, of the oxygen sublattice of the FG model. The dashed line represents all interstices, including overlapping ones, of a DRP model (Chan and Elliott, Ref. 10). Interstice size is expressed in reduced units (r.u.) of host sphere radii. For the FG model, the oxygen radius is taken to be 1.51 Å.

TABLE III. Number of true interstices per oxygen atom for models of v-SiO_2 with periodic boundary conditions. N.B. Si-containing tetrahedral interstices are excluded, but overlapping interstices are not discarded.

Model	1[a]	2[b]	3[c]	4[d]
Number per O atom	2.18	1.91	1.83	1.99

[a]Feuston and Garofalini (Ref. 40).
[b]Ching (Ref. 41).
[c]Guttman and Rahman (Ref. 42).
[d]Alvarez *et al.* (Ref. 43).

the oxygen sublattice. It can be seen quite clearly that the distribution is considerably broader for the SiO_2 model compared with the DRP model.

Associated with the interstices in the oxygen sublattice are a total of 2827 saddle-point doorways, i.e., doorways that are acute triangles. This works out to be 6.54 per O atom. This figure, too, is considerably lower than that for the DRP structure, viz., 10.79 per atom. However, out of this number of doorways, a total of $4\times216=864$ lead to a tetrahedral site containing Si atoms and are therefore not true diffusion doorways for the SiO_2 structure; thus the number of true diffusion doorways per O atoms is 4.54 (or 9.09 per unit of SiO_2). Conversely, the number of obtuse triangular "doorways" is much larger in the silica model (3.42 per O atom) than in the DRP model (0.60 per atom). The size distribution of the diffusion saddle-point doorways, i.e., saddle-point doorways excluding those leading to a Si site, is shown in Fig. 2(a). The distribution is skewed and rather broad. Figure 2(b) gives a comparison of the distribution with the result for a DRP structure. Again, in order to make the comparison meaningful, all saddle-point doorways, including those leading to a Si site, are considered in Fig. 2(b). Again, the distribution in the case of the oxygen sublattice of v-SiO_2 is considerably broader than that for the DRP structure.

The coordination polyhedra statistics of the interstices in the oxygen sublattice of the v-SiO_2 are given in Table IV. The distribution for the interstices in the oxygen sublattice is considerably broader than that for the DRP structure. Also, the dominance of fourfold sites is not as strong as in the DRP case.

During the process of diffusion, a probe atom has to pass through a saddle-point doorway when it jumps from one interstitial site to the next one. The size of the probe atom is unlikely to be larger than that of the interstitial site, since this would be too energetically costly. If the doorway is smaller than the probe, the difference in size between them will be an important consideration in the diffusion process. It is therefore interesting to investigate the ratio R of the radius of the saddle-point door to that of the interstice associated with it. In general, a saddle-point doorway has one interstice on each side of it: the three atoms defining the doorway are a subset of the four atoms equidistant from the interstice. In the case where the equidistant point does not count as an interstice because of its failure to satisfy Eq. (3), the equidistant point is promoted to be an interstice for the calculation of R. Of the two interstices on the two sides, the smaller one is chosen to calculate R because the probe is unlikely to be larger than this interstice anyway.

Results for both the silica and DRP models are presented in Fig. 3. In both distributions, there are high populations for doors with an R value close to 1.00 (a value close to 1.00 means that the door size is almost the same as that of one of its neighboring interstices). The population drops off continuously as R becomes increasingly smaller. This indicates that there is a continuous distribution from slightly degenerate interstice pairs (at $R\simeq1$) to well-separated neighboring interstice pairs. In addition to this, the curve for the DRP model [Fig. 3(b)] shows a well-defined peak at a value $R\simeq0.70$. Geometrical considerations indicate that for the case of a *regular* tetrahedral interstice in a *hard-sphere* packing, $R\simeq0.69$.

Another difference between the two distributions is that for the oxygen sublattice, the population of doors does not vanish even for values of R very near to zero. This is because when the oxygen atom radius is taken to

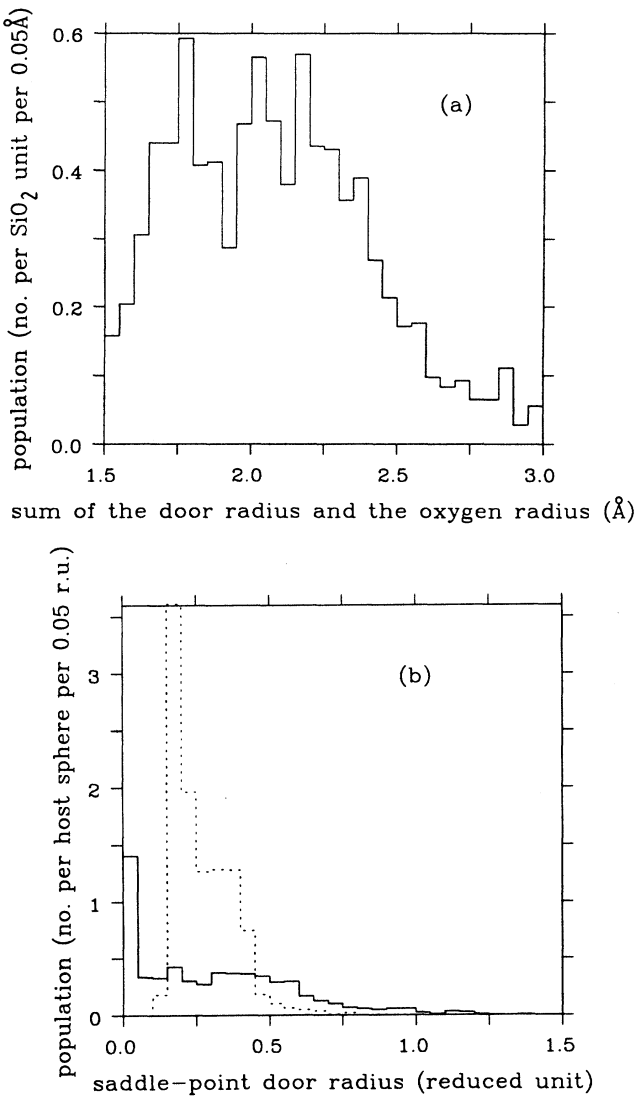

FIG. 2. Saddle-point door size distributions. (a) Saddle-point door size of the oxygen sublattice of the FG model. All doorways leading to a Si site are discarded. The door size available to a diffusing atom is the plotted size minus the radius of an oxygen atom (which could be chosen to be about 1.51 Å, refer to Table I). (b) Comparison with the results for a DRP. The solid line corresponds to the oxygen sublattice of the FG model while the dashed line corresponds to a DRP model. Unlike (a), doorways leading to a Si site are also included. The length unit for door size now used is in reduced units of host sphere radii: for the FG model, the oxygen radius is taken to be 1.51 Å. The plotted door size is the actual radius available to a diffusing atom.

TABLE IV. Interstitial coordination polyhedra statistics. Numbers marked with an asterisk include the tetrahedral interstices which contain a Si. Excluding the 216 Si-containing sites would give a total of 478 sites, which is 1.106 per atom. They occupy 15.5% of the volume of the model.

Polyhedral type (No. of vertices)	No. of polyhedra	No. per atom	Corresponding value of No. per atom in DRP	Percentage volume occupied by this type of polyhedra	Corresponding value of percentage volume in DRP
4	694*	1.606*	4.614	20.1*	73.5
5	204	0.472	0.344	14.3	12.2
6	108	0.250	0.121	12.1	7.3
7	50	0.116	0.030	8.9	2.6
8	42	0.097	0.014	9.5	1.6
9	19	0.044	0.003	5.5	0.4
10	13	0.030	0.003	4.8	0.5
11	15	0.035		6.4	
12	7	0.016		3.7	
13-16	5	0.012		3.8	
Total	1157			84.3	98.1

be 1.51 Å, some nearby oxygen atoms would overlap, resulting in a doorway of nearly zero radius. In fact, this also accounts for the fact that there is no peak around $R \simeq 0.70$ in Fig. 3(a) corresponding to those doorways leading to a Si site: the door radius (of doors leading to a Si site) is so close to zero that although the shapes of the tetrahedral sites for the Si's are almost regular, slight alterations in the shape can result in significant changes in the value of R.

Knowing the positions of the interstices in the v-SiO_2 model, one can calculate the interstice-interstice radial distribution functions (RDFs): these are shown (excluding the Si-containing sites) in Fig. 4(a), compared with the corresponding results for the DRP model in Fig. 4(b). Two features are immediately apparent: (i) the curves for the case of the v-SiO_2 are considerably more featureless than for those of the DRP model; and (ii) the contribution to the RDF at very small distances for the case of all interstices is removed for the case of nonoverlapping interstices. It should be noted that for a comparison between the two cases, one unit length in the DRP graph should correspond to a length of 1.51 Å in the v-SiO_2 graph. In addition to the interstice-interstice RDF, we have also calculated the partial RDF's between Si-containing sites and real interstices in the v-SiO_2 (Fig. 5). This turns out to be far more structured than the self-RDF of real interstices in Fig. 4(a).

Finally in this section describing the characterization of the interstice network in the oxygen sublattice of v-SiO_2 we mention the results of calculations of the percolation behavior. The critical percolation radius, such that a test particle with this radius is able to percolate freely through the interstice network, was calculated exactly according to the method outlined in Sec. IV. The critical percolation radius for a probe atom is found to be $r_p = (2.41 - R_O)$ Å, where R_O is the oxygen radius (see Table I). For an oxygen radius of 1.51 Å, this gives a critical percolation radius of 0.90 Å.

Again, for purposes of comparison with the corresponding results for the DRP structure, the critical percolation radius needs to be expressed in suitably reduced units (r.u.), scaled to the oxygen radius R_O in the case of the oxygen sublattice and the hard-sphere radius for the DRP. For the oxygen sublattice, $r_p \simeq 0.60$ r.u. (taking $R_O \simeq 1.51$ Å, $r_p = 0.60 R_O$) and for the case of the DRP, $r_p \simeq 0.25$ r.u., a considerably smaller value. Note that r_p is the same whether the Si-containing sites are considered or not, because the Si atoms occupy sites among the smallest ones and hence these sites would not control the critical percolation situation.

Figure 6 gives the site percolation graph for the oxygen sublattice. It can be noted that the solid curve (which corresponds to sites larger than the probe) and the dashed curve (which corresponds to the infinite free-volume patch) are very close together. This could be understood if one considers the free-volume situation as a function of the probe radius. The proximity of the two curves indicates that for probe radii smaller than the critical percolation radius, most sites that are large enough to accommodate the probe actually lie inside the infinite patch of free volume. This means that the effective number of solubility sites is actually very near to the number of all solubility sites calculated. Very few sites would be larger than a probe but actually not available to the probe because of blocked percolation channels. It should be noted that the site percolation graph for the DRP structure is not like this.[10] The two curves are relatively far apart. Also the fraction of sites large enough to accommodate a probe at the critical percolation radius is markedly different. For the oxygen sublattice, this is only about one-third, while for the DRP structure this is more than 90%. This means that for the DRP structure, at a probe size just above r_p, most sites are large enough to accommodate the probe, although there is still no infinite patch of free volume. In other words, there are present nonpercolating isolated patches of free volume. This situation does not occur in the oxygen sublattice.

As well as the interstitial analysis of the FG model, we

also calculated the Voronoi polyhedra statistics for the oxygen sublattice so that we can compare the packing with a DRP more thoroughly. The results are shown in Figs. 7(a) and 7(b). Similar to the interstice and doorway distributions, the distributions of the different types of Voronoi polyhedra (as classified by the number of faces) and of the different types of Voronoi faces (as classified by the number of edges) are more widely distributed than the results for the DRP.

VII. DISCUSSION

A general feature arising from the analysis given in the preceding section is that the interstice statistics of the oxygen sublattice of the structure of v-SiO_2 are considerably less regular than those for a DRP structure, even with the same equivalent packing density. This is also reflected in the fact that the critical percolation radius of a probe particle is more than twice as large (compared to the host sphere of the packing) for the case of v-SiO_2 as for a DRP structure, and is because the oxygen sublattice in v-SiO_2 is a less homogeneous packing. For the same packing density as given by Eq. (1), there is considerable overlap between neighboring oxygen atoms but not for the atoms in a DRP structure.

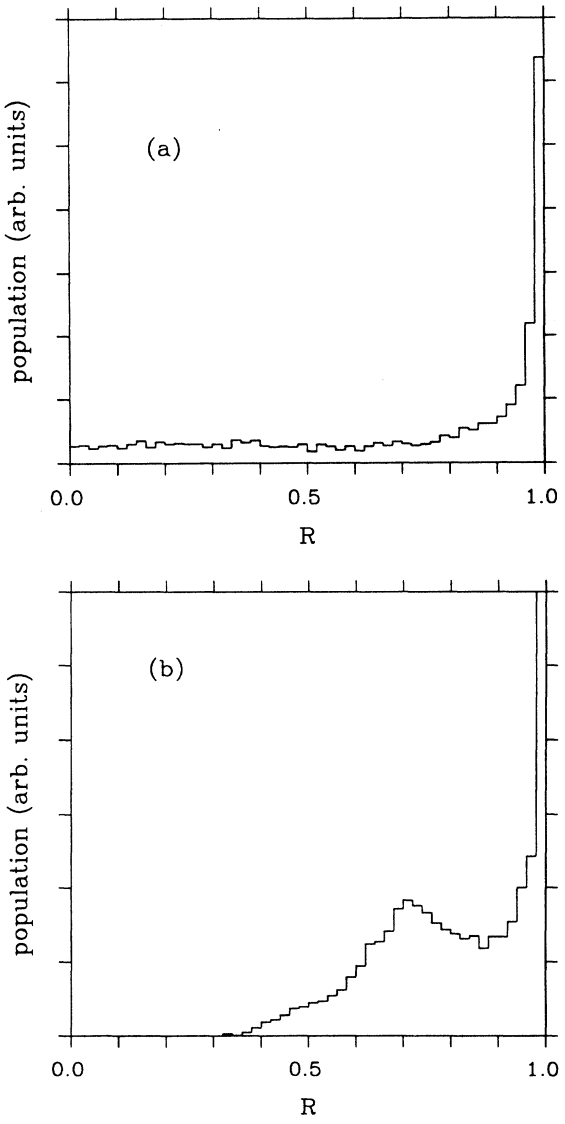

FIG. 3. Population distribution of the ratio R (the ratio of the radius of a saddle-point door to that of its adjacent interstice) (a) for the oxygen sublattice of the FG model (all doors, including those leading to a Si site, are included); (b) for a DRP model.

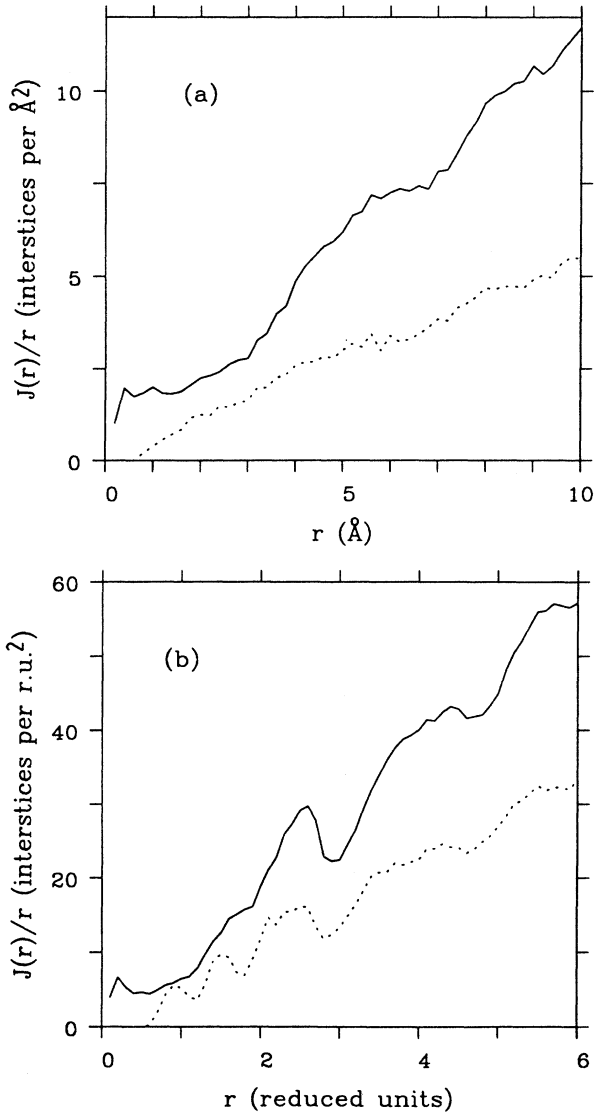

FIG. 4. Interstice RDF. The RDF divided by the distance $J(r)/r$ is plotted against the distance r. The solid line represents interstices including overlapping ones, while the dashed line represents nonoverlapping interstices only. (a) Interstices, excluding Si-containing ones, of the oxygen sublattice of the FG model. (b) Interstices of a DRP model (reproduced from Chan and Elliott, Ref. 10). r is in reduced units (r.u.) of host sphere radius. For comparison, the oxygen (host sphere) radius in (a) may be taken as 1.51 Å.

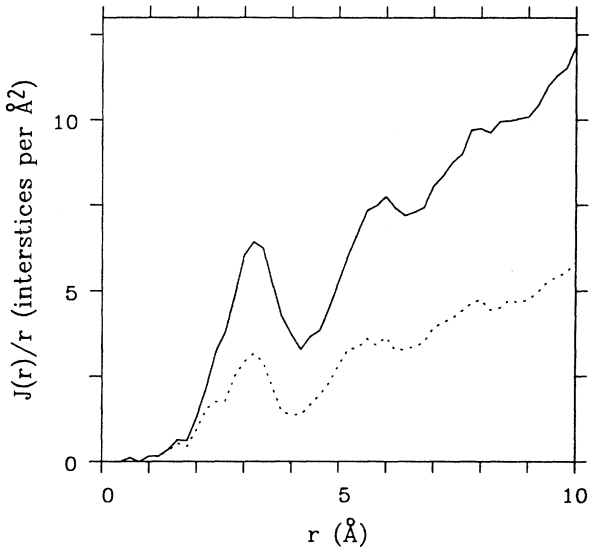

FIG. 5. Si-containing interstice–real interstice partial RDF. The oxygen sublattice of the FG model is considered. The solid line represents all real interstices while the dashed line represents nonoverlapping interstices only.

The distribution of interstice sizes is rather broad and asymmetric in shape (see Fig. 1). Shackelford and Masaryk[29] have speculated that this probability distribution could be described in terms of a log-normal function, and they have constructed such a curve on the basis of two data points in the high-r tail of the distribution (viz. the concentration of sites available to He and Ne atoms, i.e., those with sizes greater than those of the rare-gas atoms—see Table II), together with an estimate for the total number of interstitial sites (scaled up from that for cristobalite). The distribution so obtained was characterized by having its mode at 1.81 Å and mean at 1.96 Å. In obtaining the fit, they took the interstice size to be the sum of the oxygen radius and the probe radius. Hence the interstices with a size smaller than the oxygen radius will not be able to accommodate any probe atom. On the other hand, in the present analysis, it is found that if the oxygen radius (taken to be 1.51 Å) is excluded from the interstice size, the nonoverlapping interstice size distribution of the FG model can be well fitted by a log-normal distribution (see Fig. 8), having its mode at $r=0.41$ Å.

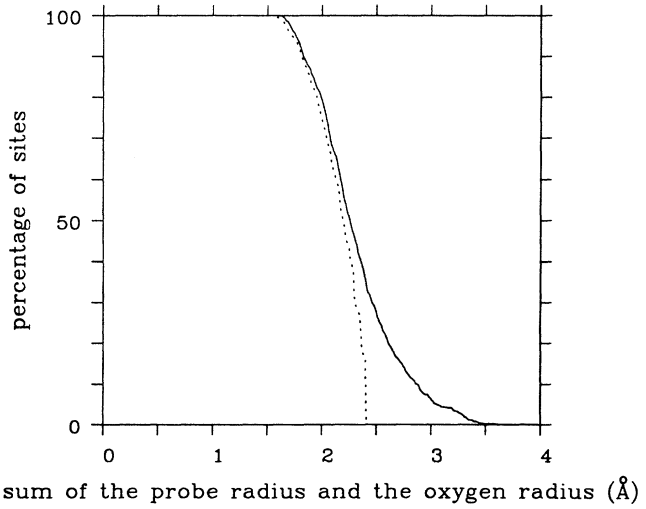

FIG. 6. Percolation graph of the oxygen sublattice of the FG model. The percentage of interstitial sites (including overlapping ones) is plotted against the sum of the radii of the probe and the oxygen atom. The solid line represents sites that are larger than the probe, while the dashed line represents the sites lying in the infinite patch of free volume.

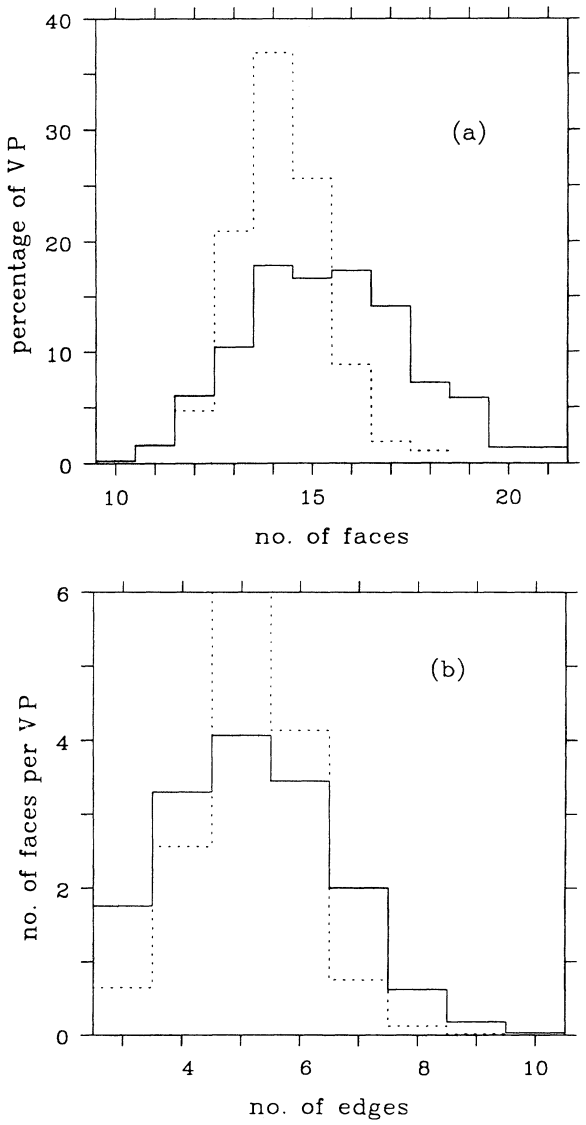

FIG. 7. Voronoi polyhedra (VP) statistics. The solid line refers to the FG model while the dashed line refers to a DRP model. (a) Distribution of different types (by the number of faces) of VP. (b) Distribution of different types (by the number of edges) of VP faces.

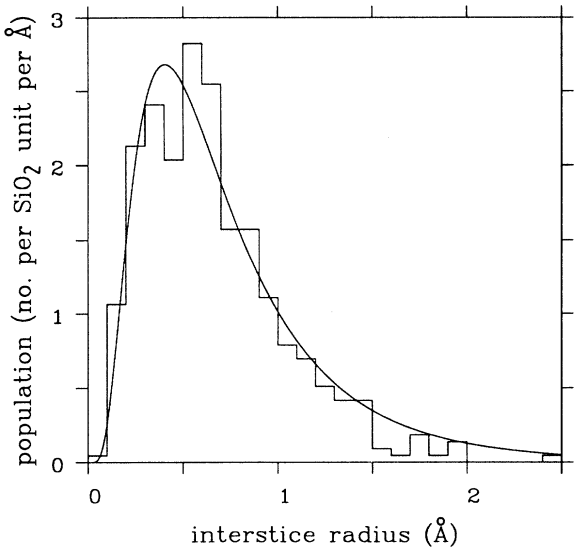

FIG. 8. Interstice (nonoverlapping ones) size distribution of the FG model fitted by a log-normal curve. The oxygen radius is assumed to be 1.51 Å. The fitting curve is

$$y=2.68\ \exp\left[-\left[\frac{\ln(x/0.405)}{0.917}\right]^2\right].$$

The results of this theoretical investigation into the interstice statistics of v-SiO_2 can only be compared with experimental data in rather a limited fashion; such a comparison is effectively restricted to that with experimental estimates obtained from solubilities of various rare gases (see Table II). Theoretical estimates for the concentrations N_S of those (nonoverlapping) interstitial sites with sizes larger than a given value in the structures of the various models of v-SiO_2 examined in this study can only be made by assuming a value for the oxygen radius R_O. Estimates so obtained for two of the structural models examined, viz., the FG model and the model by Gladden[16] are given in Table V, together with the representative experimental values adopted by Shackelford[31–33] and also the theoretical estimates obtained by Mitra and Hockney[12] from an analysis of their molecular-dynamics model. It can be seen that there is very reasonable agreement between the theoretical values for N_S obtained for the structural models and the experimental estimates obtained from gas-solubility measurements, particularly bearing in mind the model-dependent assumptions made in extracting values of N_S from the experimental data (see Sec. III). Agreement between theory and experiment is particularly good for the larger value of R_O, viz., 1.60 Å. However, this agreement cannot safely be used to infer that the appropriate value for the oxygen radius in v-SiO_2 is $R_O \simeq 1.60$ Å because of the uncertainties in the experimental estimates alluded to above. It should also be noted that the estimates for N_S obtained by Mitra and Hockney[12] for the MD model of Mitra *et al.*[44] are appreciably higher than those obtained in this study for the same value of R_O. This discrepancy may be due to differences in the algorithm used to identify interstices in the oxygen framework and also may be a consequence of subtle differences between the structures of the models.

TABLE V. Comparison of the theoretical rare-gas solubility concentrations for v-SiO_2 for various values of the oxygen radius compared with the experimental values adopted by Shackelford (Refs. 31–33).

	He	Ne
R_{min} (Å)	1.28	1.38
	N_S (10^{21} cm^{-3})	
R_O (Å)		
1.6	2.8[a]	1.6[a]
	2.8[b]	1.7[b]
	3.4[c]	2.6[c]
1.5	3.8[a]	2.7[a]
	3.8[b]	2.8[b]
Expt.	2.3	1.3

[a]Feuston-Garofalini model (Ref. 40).
[b]Gladden model (Ref. 16).
[c]Value obtained by Mitra and Hockney on a molecular-dynamics model (Ref. 12).

VIII. CONCLUSIONS

An algorithm recently developed to investigate the interstice statistics in dense random packings of spheres in terms of the free volume has been used to study the interstice statistics in the oxygen sublattice of the archetypal glass former, viz., silica. Several structural models of v-SiO_2 have been investigated. The distributions of the interstices and the saddle-point doorways are much broader than the corresponding distributions for DRP models. The nonoverlapping interstice size distribution of such models has been found to be rather accurately fitted by a log-normal probability function. The critical percolation radius of the model of Feuston and Garofalini[40] was found to be 2.41 Å minus the oxygen radius. The concentrations of interstitial sites in these models with radii greater than a given size have been computed and these have been compared with the results of noble-gas solubility measurements; agreement is very reasonable.

ACKNOWLEDGMENTS

The authors would like to thank Dr. B. P. Feuston, Dr. S. H. Garofalini, Dr. L. F. Gladden, Dr. W. Y. Ching, Dr. L. Guttman, Dr. S. M. Rahman, and Dr. L. J. Alvarez for their kindness in providing the silica models. Also one of the authors (S.L.C.) would like to thank the Croucher Foundation for support.

[1]J. D. Bernal, Proc. R. Soc. London Ser. A **280**, 299 (1964).
[2]J. L. Finney, Proc. R. Soc. London Ser. A **319**, 479 (1970).
[3]C. H. Bennett, J. Appl. Phys. **43**, 2727 (1972).
[4]E. J. W. Whittaker, J. Non-Cryst. Solids **28**, 293 (1978).
[5]J. H. Finney and J. Wallace, J. Non-Cryst. Solids **43**, 165 (1981).
[6]M. Ahmadzadeh and B. Cantor, J. Non-Cryst. Solids **43**, 189 (1981).
[7]H. J. Frost, Acta Metall. **30**, 889 (1982).
[8]F. Lançon, L. Billard, and A. Chamberod, J. Phys. F **14**, 579 (1984).
[9]R. P. Bywater and J. L. Finney, J. Theor. Biol. **105**, 333 (1983).
[10]S. L. Chan and S. R. Elliott, J. Non-Cryst. Solids **124**, 22 (1990).
[11]M. Popescu, J. Non-Cryst. Solids **35-36**, 549 (1980).
[12]S. K. Mitra and R. W. Hockney, J. Phys. C **13**, L739 (1980).
[13]W. H. Zachariasen, J. Am. Chem. Soc. **54**, 3841 (1932).
[14]F. L. Galeener, in *The Physics and Technology of Amorphous SiO_2*, edited by R. A. B. Devine (Plenum, New York, 1988), p. 1.
[15]R. J. Bell and P. Dean, Philos. Mag. **25**, 1381 (1972).
[16]L. F. Gladden, J. Non-Cryst. Solids **119**, 318 (1990).
[17]P. H. Gaskell, J. Phys. (Paris) Colloq. **43**, C9-101 (1982).
[18]M. C. Eckersley and P. H. Gaskell, J. Non-Cryst. Solids **95-96**, 31 (1987).
[19]Y. T. Thathachari and W. A. Tiller, J. Appl. Phys. **53**, 8615 (1982).
[20]Y. T. Thathachari and W. A. Tiller, J. Appl. Phys. **57**, 1805 (1985).
[21]F. L. Galeener, Philos. Mag. B **51**, L1 (1985).
[22]R. L. Mozzi and B. E. Warren, J. Appl. Cryst. **2**, 164 (1969).
[23]L. F. Gladden, T. A. Carpenter, and S. R. Elliott, Philos. Mag. B **53**, L81 (1986).
[24]A. Bondi, J. Phys. Chem. **68**, 441 (1964).
[25]P. L. Studt, J. F. Shackelford, and R. M. Fulrath, J. Appl. Phys. **41**, 2777 (1970).
[26]J. S. Masaryk and R. M. Fulrath, J. Chem. Phys. **59**, 1198 (1973).
[27]J. E. Shelby, J. Appl. Phys. **47**, 135 (1976).
[28]J. E. Shelby, S. C. Keeton, and J. J. Iannucci, J. Appl. Phys. **47**, 3952 (1976).
[29]J. F. Shackelford and J. S. Masaryk, J. Non-Cryst. Solids **30**, 127 (1978).
[30]J. E. Shelby, *Treatise on Materials Science and Technology, Vol. 17, Glass II* (Academic, New York, 1979), p. 1.
[31]J. F. Shackelford, J. Non-Cryst. Solids **42**, 165 (1980).
[32]J. F. Shackelford, J. Non-Cryst. Solids **49**, 299 (1982).
[33]J. F. Shackelford, in *Structure and Bonding in Non-Crystalline Solids*, edited by G. E. Walrafen and A. G. Revesz (Plenum, New York, 1986), p. 237.
[34]J. E. Shelby, J. Appl. Phys. **48**, 3387 (1977).
[35]R. M. Barrer and D. E. W. Vaughan, Trans. Faraday Soc. **63**, 2275 (1967).
[36]J. F. Shackelford, P. L. Studt, and R. M. Fulrath, J. Appl. Phys. **43**, 1619 (1972).
[37]N. F. Mott, Philos. Mag. B **55**, 117 (1987).
[38]F. Rochet, S. Rigo, M. Froment, C. d'Anterroches, C. Maillot, H. Roulet, and G. Dufour, Adv. Phys. **35**, 237 (1987).
[39]O. L. Anderson and D. A. Stuart, J. Am. Ceram. Soc. **37**, 573 (1954).
[40]B. P. Feuston and S. H. Garofalini, J. Chem. Phys. **89**, 5818 (1988).
[41]W. Y. Ching, Phys. Rev. B **26**, 6610 (1982). (The 162-atom model is used here.)
[42]L. Guttman and S. M. Rahman, Phys. Rev. B **37**, 2657 (1988). (The model corresponding to relaxation parameters $\beta/\alpha=0.5$ and $\gamma/\alpha=0.3$ and cell edge $=0.993\,25$ is used here.)
[43]L. J. Alvarez, A. S. Alavi, I. R. McDonald, and S. R. Elliott (unpublished).
[44]S. K. Mitra, M. Amini, D. Fincham, and R. W. Hockney, Philos. Mag. B **43**, 365 (1981).